

Charge distributions of nitro groups within organic explosive crystals – effects on sensitivity and modelling

Alexander A. Aina¹, Alston J. Misquitta², Max Phipps³, Sarah L Price^{1}*

¹Department of Chemistry, University College London, 20 Gordon Street, London WC1H 0AJ, U.K.

² School of Physics and Astronomy, Queen Mary, University of London, 327 Mile End Road, London, E1 4NS UK

³Atomic Weapons Establishment, Aldermaston, Reading, Berkshire, RG7 4PR, U.K.

Supporting Information

Table of Contents

I.	ROTATING MULTIPOLES FOR BOTH ORIENT AND DMACRYS CALCULATIONS	2
II.	DIFFERENCES IN OPTIMIZED AND EXPERIMENTAL CONFORMATIONS OF RDX CONTRASTED WITH TNT	3
III.	SURVEY OF CAMBRIDGE STRUCTURAL DATABASE	5
IV.	DETAILS OF CHANGES IN ELECTROSTATIC PROPERTIES WITH CONFORMATION	6
V.	EFFECTS OF ROTATING NITRO-GROUPS IN TNB, HNB AND RDX (AAE).....	7
VI.	LATTICE ENERGY MINIMIZATIONS	10
VII.	REFERENCES.....	14

I. ROTATING MULTIPOLES FOR BOTH ORIENT AND DMACRYS CALCULATIONS

The ORIENT¹ program can transform the iterated stockholder atoms^{2, 3} (ISA) distributed multipoles of a molecule (originally calculated in the global axis frame of the molecule) into the atomic local axes of the molecule as defined in **Figure S1**.

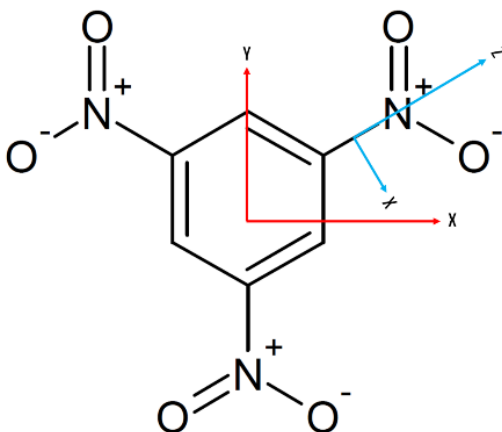


Figure S1. An example of the global (molecule fixed) axis (red) and local axis (blue) definitions used in this study. In the global axis frame, z is perpendicular to the ring plane, thus the π orbitals give a significant Q_{20} moment (c.f. the dz^2 orbital). When the quadrupole tensor is rotated into the local axis, the z axis is now along the bond, hence the Q_{20} moment is in the ring plane and has a very different value, with the π orbitals being represented by Q_{22s} .

This is done by analytically rotating the global multipoles into the local axis frame. The molecular geometry and the user defined local axes must first be defined. The multipole moments calculated in the global axis are then analytically rotated into this user defined local axis.

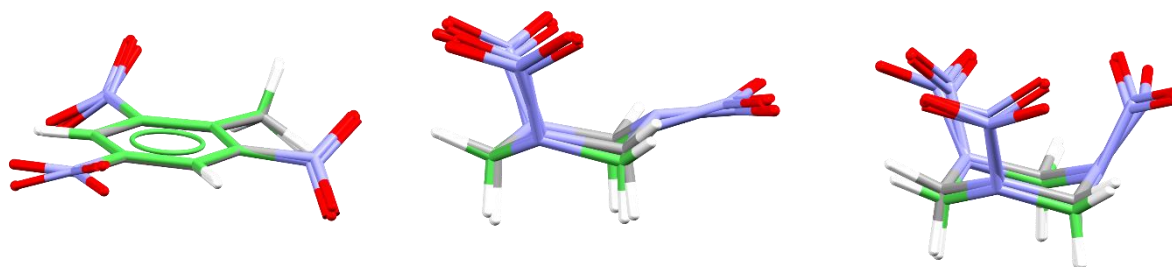
$$Q_{lk}^{(L)} = \sum_m Q_{lm}^{(G)} D_{mk}^l(\Omega)$$

1

II. DIFFERENCES IN OPTIMIZED AND EXPERIMENTAL CONFORMATIONS OF RDX CONTRASTED WITH TNT

Overlays of experimental conformations, the PBE0/aug-cc-pVTZ⁴⁻⁷ optimized conformations, and the conformations with only the NO₂ angles rotated (*optexptNO₂*) are shown in **Figure S2**, to illustrate the changes that accompany nitro-group rotation. In the AAE conformation of RDX, the equatorial NO₂ moves more into the plane of the ring, as the aliphatic ring is more open for the isolated molecule, possibly due to repulsion from lone pairs on the ring sp³ nitrogens, that are not being counteracted by crystal packing forces. A similar change in the aliphatic ring conformation and nitrogens in the axial NO₂ groups is seen for the AAA conformation, therefore, it is not possible to consistently analytically rotate the nitro-group multipole moments. While these changes may not look severe, we can see by a comparison of differences in cell parameters, RMSD₁₅ values and lattice energies between using the experimental and optimized molecular conformations in **Table S4** that these differences result in very different minima. In contrast, the aromatic ring in the optimized and experimental conformations of the nitro-aromatic TNT is unchanged, with only small methyl group rotation (**Figure S2**), meaning analytical rotation is feasible. **Table S3** shows that although there is a significant difference in the nitro groups, which does have a major effect on the crystal packing, changing the nitro- torsion angles to the experimental values can result in a good reproduction of the structure.

optimized (grey) vs experimental (green)

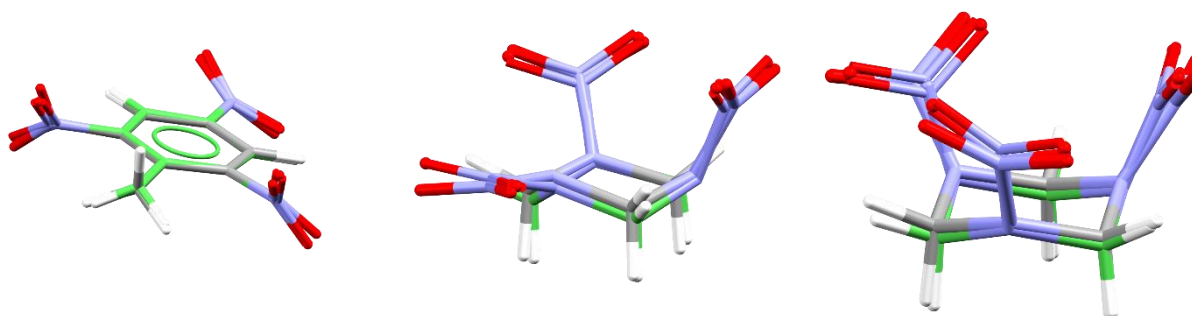


TNT, $RMSD_1 = 0.199 \text{ \AA}$

RDX (AAE), $RMSD_1 = 0.182 \text{ \AA}$

RDX (AAA), $RMSD_1 = 0.379 \text{ \AA}$

optexptNO₂ (grey) vs experimental (green)



TNT, $RMSD_1 = 0.152 \text{ \AA}$

RDX (AAE), $RMSD_1 = 0.185 \text{ \AA}$

RDX (AAA), $RMSD_1 = 0.287 \text{ \AA}$

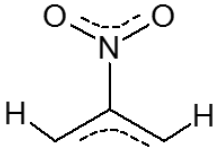
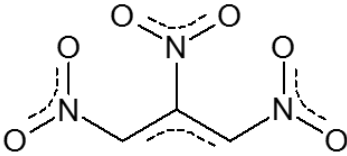
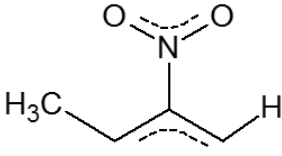
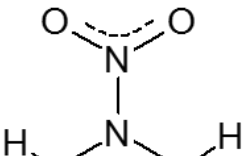
Figure S2. Overlay of experimental crystalline conformation (green) of TNT Form I (molecule A/ZZZMUC08⁸), RDX α (AAE/CTMTNA03⁹) and ϵ (AAA/CTMTNA06¹⁰) with their PBE0/aug-cc-pTVZ optimized structures (green). The row below are the overlays of the experimental conformations (green) and the optimized conformations with experimental NO₂ torsion angles, *optexptNO₂* (grey).

III. SURVEY OF CAMBRIDGE STRUCTURAL DATABASE

Distribution curves illustrating the occurrence of each *O-N-X-C* torsion in a specific chemical environment (for example, an NO₂ adjacent to two hydrogens or a methyl group in an aromatic ring) were generated using an in-house python program developed by Luca Iuzzolino for determining the possible torsion angles that could be adopted in crystal structures based on the torsion angle statistics of all 870,000+ molecules in the Cambridge Structural Database (CSD).¹¹

The specific NO₂ fragments using in this study are as follows

Table S1. The NO₂ fragments that were searched for within the CSD

			
aromatic C-NO ₂ adjacent hydrogens (TNB, para-NO ₂ TNT)	aromatic C-NO ₂ adjacent NO ₂ s (HNB)	aromatic C-NO ₂ adjacent a hydrogen and a methyl group (ortho- NO ₂ TNT)	aliphatic N-NO ₂ adjacent hydrogens (RDX)

The occurrence of each torsion angle (rounded to the nearest degree) was plotted in the histograms.

IV. DETAILS OF CHANGES IN ELECTROSTATIC PROPERTIES WITH CONFORMATION

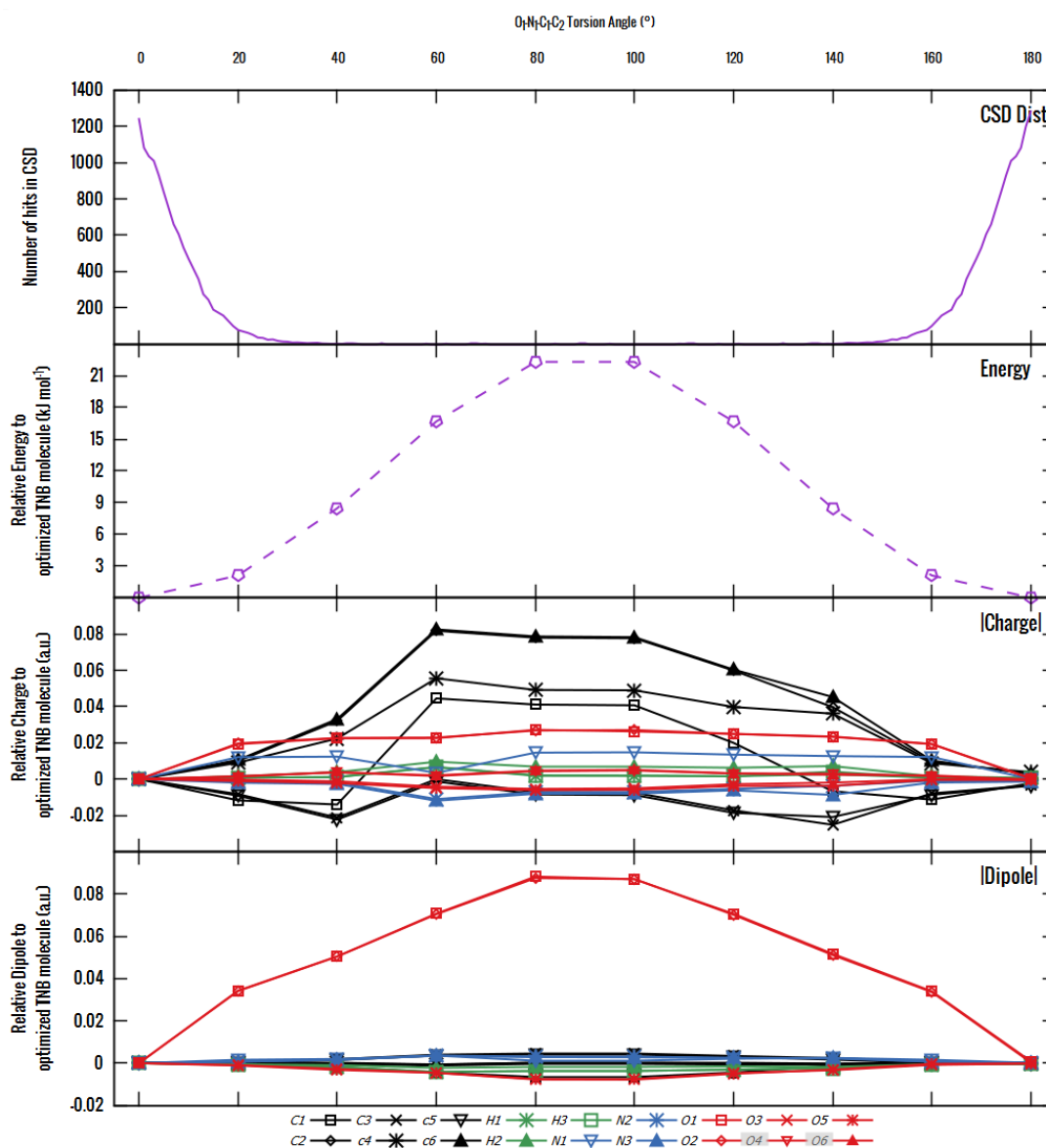
Table S2. A comparison of electrostatic properties of the 4 explosives and experimental impact sensitivities ($h_{50\%}$)

Molecule	TNB (TNBENZ)			HNB	TNT			RDX			
Polymorph	13 (III)	11 (I)	12 (II)	HNOBEN	ZZZMUC08 (α)			CTMTNA03 (α)		CTMTNA06 (ϵ)	
Molecule	Opt	Mol 1	Mol 2	Opt	Opt	Mol 1	Mol 2	Opt	Expt	Opt	Expt
Q_X^{min}	-0.0289	-0.0145	-0.0213	0.000305	-0.154	-0.0938	-0.0873	-0.352	-0.350	-0.355	-0.383
Q_X^{max} /eV	-0.0278	-0.00378	-0.0203	0.00266	-0.0481	0.0303	0.0105	-0.329	-0.318	-0.353	-0.373
Q_N^{min}	0.797	0.796	0.796	0.749	0.820	0.774	0.777	0.906	0.882	0.907	0.928
Q_N^{max} /eV	0.799	0.810	0.798	0.750	0.852	0.811	0.811	0.943	0.902	0.908	0.945
V_{mid}/eV^1	1.044	1.093	1.054	1.016	0.948	0.999	0.981	0.819	0.759	0.789	0.783
V_{mid}/eV^2	1.045	1.093	1.054	1.016	1.051	1.098	1.074	0.852	0.857	0.792	0.836
$V_{mid,avg}$ /eV	1.044	1.071	1.052	1.016	0.982	1.021	1.007	0.828	0.792	0.790	0.816
V_{min}/eV	-0.49	-0.60	-0.49	-0.26	-0.72	-0.79	-0.74	-0.73	-0.84	-0.81	-1.00
V_{max}/eV	0.91	0.76	0.91	1.13	0.59	0.59	0.61	1.45	1.63	1.46	1.57
$h_{50\%}$ /cm ⁻¹	71 ¹² (100 ¹³)			11 ¹²	98 ¹² (160 ¹⁴ , 107 ¹²)			28 ¹⁵ (24, 26 ¹⁶)			

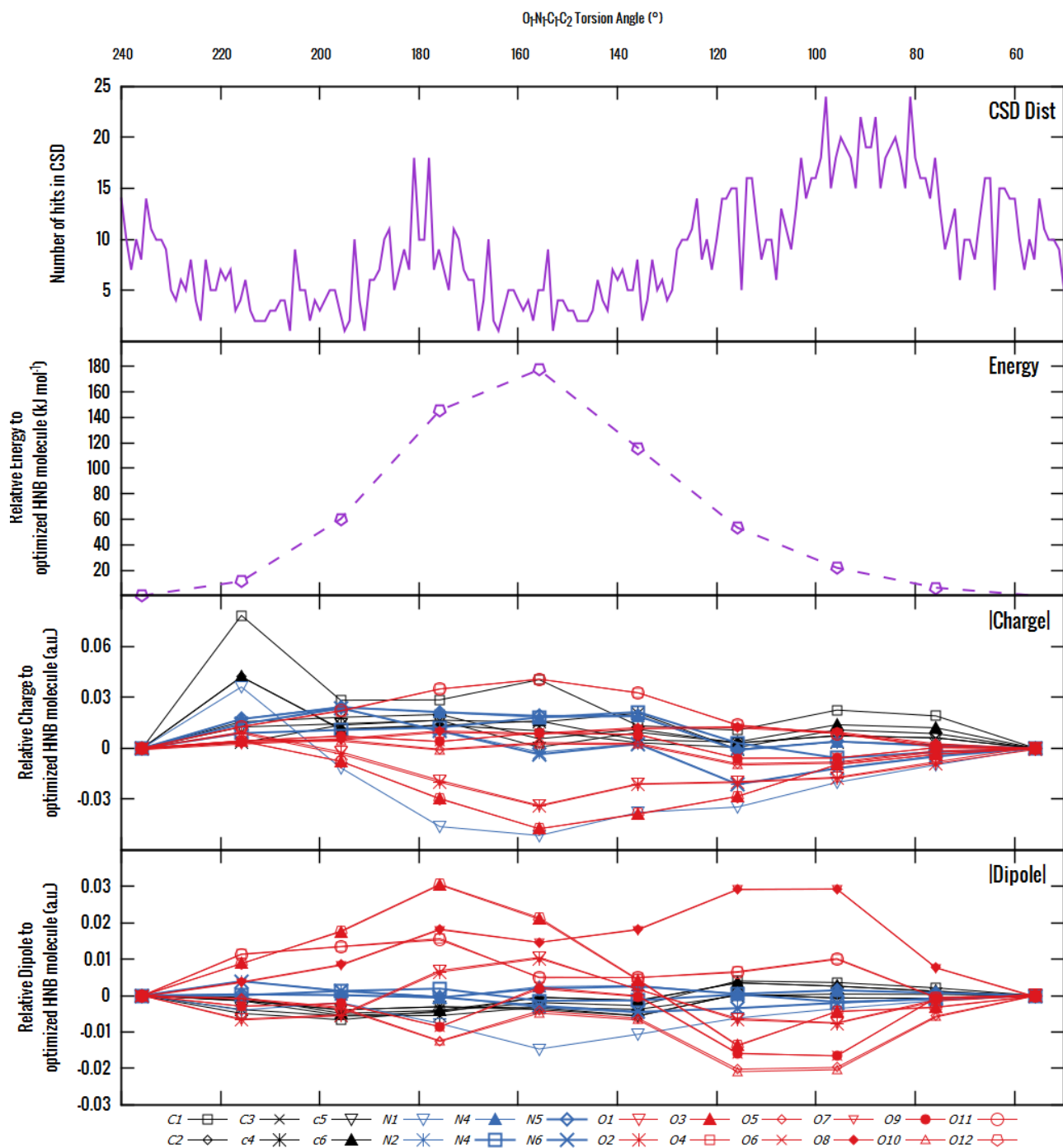
The optimized isolated structures and the most stable experimental conformations within the polymorphs were used. In RDX this is the AAE conformation in CTMTNA03, and the AAA conformation in CTMTNA06. The range of Q_X (X is either C or N, the atom connected to the nitro-group) and Q_N is the min and max values from the 3NO₂ groups (6 for HNB). The impact sensitivity used is given with other impact sensitivity determinations in brackets; for RDX the polymorph used is not specified, thus it is probable that the impact sensitivity of the ϵ form is very different from literature values, if the experiments used the most stable α form.¹ V_{mid} of the longest bond. ²The trigger bond with the most positive V_{mid} .

V. EFFECTS OF ROTATING NITRO-GROUPS IN TNB, HNB AND RDX (AAE)

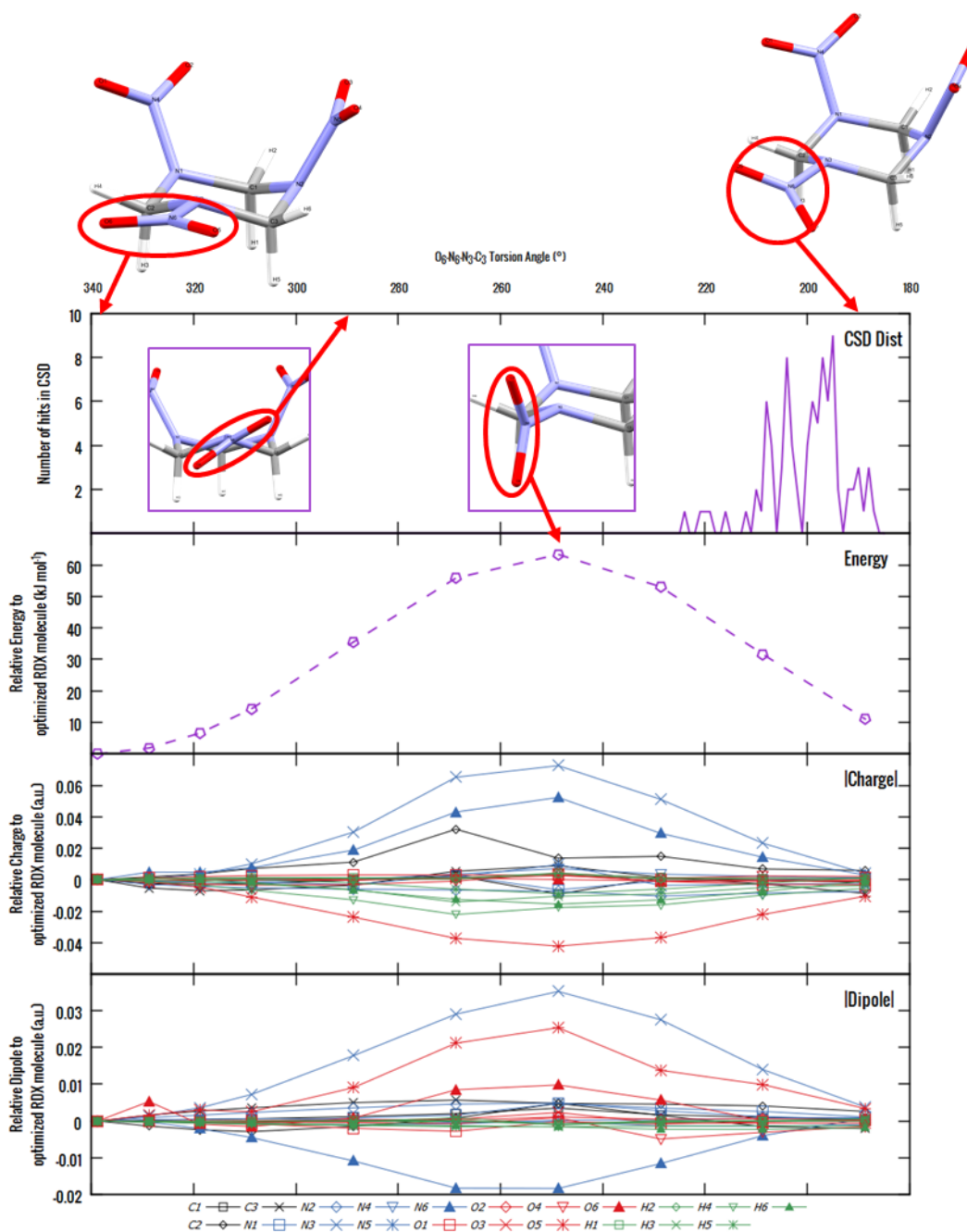
The relative changes of the charge and dipole moment magnitudes with NO₂ torsion angle are compared with Cambridge Structure Database (CSD) distributions and the intramolecular energy relative to the optimized isolated molecular structure for the molecules where this data is not given in the manuscript.



(a) TNB



(b) HNB



(c) RDX-AAE

Figure S3. Conformational behavior of TNB (a), HNB (b) and RDX-AAE (c) as their NO₂ torsion angles are changed. Only the equatorial NO₂ in RDX (c) is rotated. The behaviors as a function of angle are given for (top to bottom) the CSD distribution of observed angles for this group; the change in PBE0/aug-cc-VTZ energy relative to the optimized molecule as only the nitro group torsion angle is changed; and the variation in the ISA charge and dipole on each atom.

VI. LATTICE ENERGY MINIMIZATIONS

Table S3: A comparison of lattice energy minimizations of the nitro-aromatics for each conformation

Str (REFCODE)		TNT (ZZZMUC08 (Form I))			
	expt	xminexpt	xminopt	xminoptexptNO2	xminanarot
$a/\text{\AA}$	14.911	14.982	14.209	14.854	14.814
$b/\text{\AA}$	6.034	6.079	7.397	6.135	6.119
$c/\text{\AA}$	20.882	20.774	19.386	21.078	21.148
$n(RMSD_{15})/\text{\AA}$	~	15 (0.064)	3 (0.683)	15 (0.246)	14 (0.214)
$U_{INT} (kJ mol^{-1})$		-117.6	-100.4	-121	-123.2
Str (REFCODE)		TNB (TNBENZ13 (Form III))			
	expt	xminexpt	xminopt	xminoptexptNO2	xminanarot
$a/\text{\AA}$	12.896	12.833	12.751	12.779	12.781
$b/\text{\AA}$	5.723	5.871	5.603	5.743	5.757
$c/\text{\AA}$	11.287	11.038	11.667	11.414	11.393
$n(RMSD_{15})/\text{\AA}$	~	15 (0.154)	15 (0.245)	15 (0.166)	15 (0.162)
$U_{INT} (kJ mol^{-1})$		-112.6	-111.8	-104.7	-104.4
Str (REFCODE)		HNB (HNOBEN (Form I))			
	expt	xminexpt	xminopt	xminoptexptNO2	xminanarot
$a/\text{\AA}$	13.22	12.822	12.960	12.768	12.760
$b/\text{\AA}$	9.13	8.978	8.792	8.812	8.817
$c/\text{\AA}$	9.68	9.442	9.517	9.558	9.553
$n(RMSD_{15})/\text{\AA}$	~	15 (0.170)	15 (0.214)	15 (0.235)	15 (0.237)
$U_{INT} (kJ mol^{-1})$		-146.1	-144.6	-150.1	-150.8

A comparison of the expt (experimental structure), xminexpt (DMACRYS¹⁷ minimized crystal structure, with all molecules held rigid in their experimentally observed conformations), xminopt (DMACRYS minimized crystal structure, with all molecules held rigid in their gas-phase optimized conformation), xminoptexptNO₂ (DMACRYS minimized optimized structure with experimental NO₂ torsions using ψ computed after rotation) and the xminanarot (DMACRYS minimized optimized structure with experimental NO₂ torsions using analytically rotated multipole moments) crystal structures and intermolecular lattice energies of TNT, TNB and HNB. The intermolecular lattice energy (U_{INT}) estimates above are calculated using a distributed multipole electrostatic force-field derived from the molecular (PBE0/aug-cc-pVTZ) wave-function and empirical repulsion-dispersion model; the empirical FIT potential¹⁸ & ISA² (PBE0/aug-cc-pVTZ). The $RMSD_{15}$ values have been calculated against each respective experimental determination.

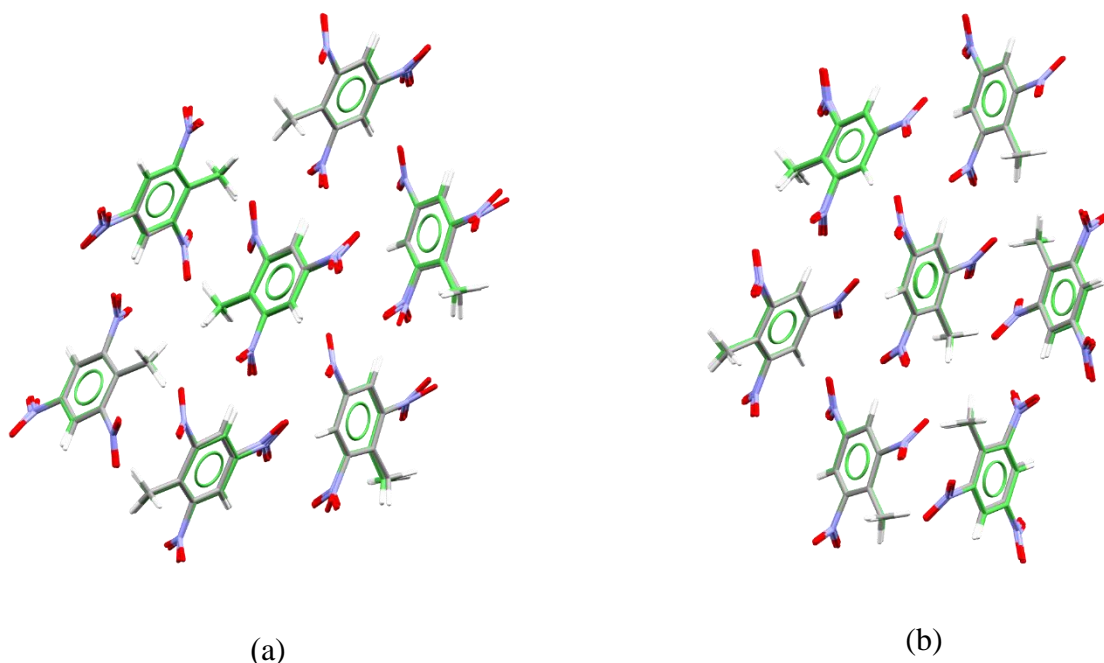


Figure S4. Overlay of the experimental ZZZMUC08⁸ structure (green) and their DMACRYS minimized structures using the molecular conformations and distributed multipole moments:

- (a) calculated for the PBE0/aug-cc-pVTZ optimized structure after rotating all NO₂ groups into their experimental observed torsion angles, *optexptNO₂* (grey). $RMSD_{15} = 0.246\text{\AA}$
- (b) calculated for the PBE0/aug-cc-pVTZ optimized structure and then analytically rotated (*anarot*) into the experimental observed NO₂ torsion angles (grey). $RMSD_{14} = 0.214\text{\AA}$

Figure S4 shows that even for TNT, which has the greatest differences in optimized and observed NO₂ torsion angles, analytical rotation of the atomic multipoles into the experimental NO₂ torsion angles and recalculation of the wave-function for each NO₂ torsion angle results in very small structural differences. The only significant differences are seen in the intermolecular energies (**Manuscript Table 1 & Table S3**).

Table S4 and **Figure S5** highlight the differences between the experimental and optimized conformations of RDX and how it would be inappropriate to use molecular charge distribution models derived from the optimized structure to predict experimental crystal properties such as lattice energy or cell geometries.

Table S4. A comparison of lattice energy minimizations of the nitramine RDX for both AAE and AAA conformations

Structure REFCODE	RDX					
	CTMTNA03 (Form α)			CTMTNA06 (Form ϵ)		
	Expt	xminexpt	xminopt	Expt	xminexpt	xminopt
$a/\text{\AA}$	11.420	11.635	11.540	7.032	7.371	7.715
$b/\text{\AA}$	10.586	10.615	10.561	10.530	11.113	12.120
$c/\text{\AA}$	13.140	13.426	13.787	8.791	9.673	9.194
$n(RMSD_{15})/\text{\AA}$	~	15 (0.169)	15 (0.447)	~	15 (0.431)	7 (0.857)
$U_{INT} (kJ mol^{-1})$	~	-121.1	-121.1	~	-118.9	-93.4

A comparison of the expt (experimental structure), xminexpt (DMACRYS¹⁷ minimized crystal structure, with all molecules held rigid in their experimentally observed conformations) and xminopt (DMACRYS minimized crystal structure, with all molecules held rigid in their gas-phase optimized conformation) crystal structures and intermolecular lattice energies of RDX. The intermolecular lattice energy (U_{INT}) estimates above are calculated using a distributed multipole electrostatic force-field derived from the molecular (PBE0/aug-cc-pVTZ) wave-function and empirical repulsion-dispersion model; the empirical FIT potential¹⁸ & ISA² (PBE0/aug-cc-pVTZ). This highlights how slight differences in the experimentally observed and optimized conformations of both polymorphs of RDX can result in large changes in intermolecular energy. $RMSD_{15}$ against each respective experimental determination.

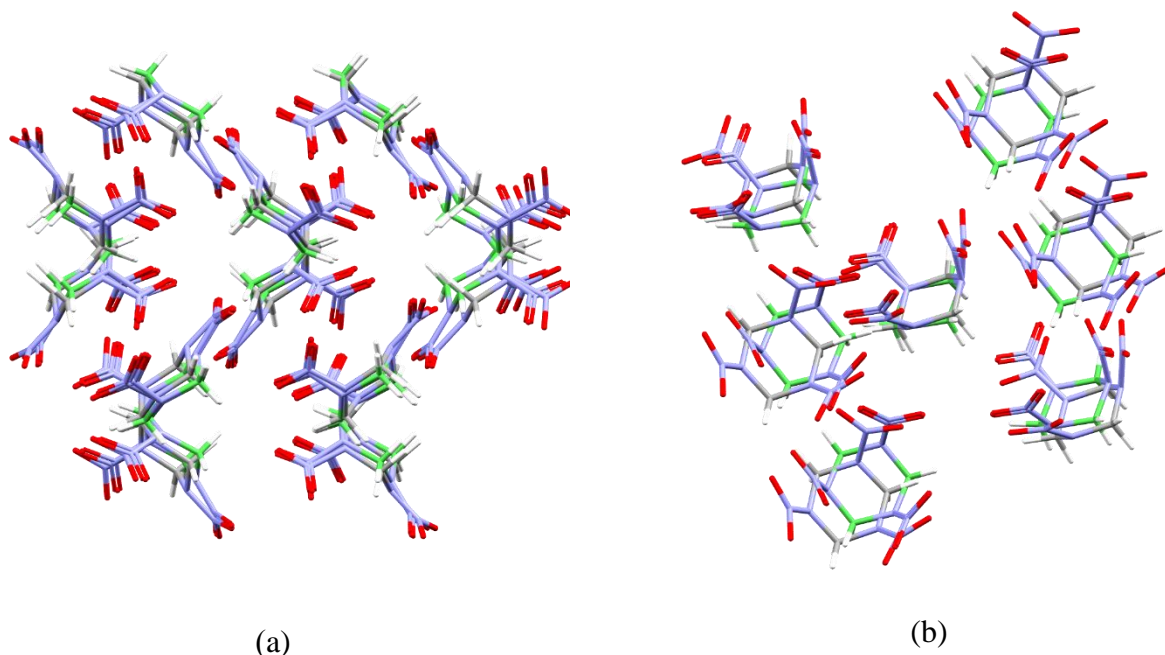


Figure S5. Overlay of the experimental structures of RDX (green), CTMTNA03⁹ (a) and CTMTNA06¹⁰ (b) and their DMACRYS minimized structures using the molecular conformations and distributed multipole moments:

(a) calculated for the PBE0/aug-cc-pVTZ optimized AAE conformation in the crystal, *xminopt* (grey). $RMSD_{15} = 0.447\text{\AA}$

(b) calculated for the PBE0/aug-cc-pVTZ optimized AAA conformation in the crystal, *xminopt* (grey). The *xminopt* crystal minimizes to a very different minima and energy compared to the experimental lattice (*xminexpt*), with only 7 molecules out of 15 matching and a high RMSD value. $RMSD_7 = 0.857\text{\AA}$.

VII. REFERENCES

1. Stone, A. J.; Dullweber, A.; Engkvist, O.; Frascini, E.; Hodges, M. P.; Meredith, A. W.; Nutt, D. R.; Popelier, P. L. A.; Wales, D. J. *ORIENT: a program for studying interactions between molecules*, 4.8.29; University of Cambridge, 2015.
2. Misquitta, A. J.; Stone, A. J.; Fazeli, F., Distributed Multipoles from a Robust Basis-Space Implementation of the Iterated Stockholder Atoms Procedure. *Journal of Chemical Theory and Computation* **2014**, *10* (12), 5405-5418.
3. Lillestolen, T. C.; Wheatley, R. J., Atomic charge densities generated using an iterative stockholder procedure. *Journal of Chemical Physics* **2009**, *131* (14), 144101.
4. Adamo, C.; Barone, V., Toward reliable density functional methods without adjustable parameters: The PBE0 model. *Journal of Chemical Physics* **1999**, *110* (13), 6158-6170.
5. Perdew, J. P.; Emzerhof, M.; Burke, K., Rationale for mixing exact exchange with density functional approximations. *Journal of Chemical Physics* **1996**, *105* (22), 9982-9985.
6. Perdew, J. P.; Burke, K.; Ernzerhof, M., Generalized gradient approximation made simple. *Physical Review Letters* **1996**, *77* (18), 3865-3868.
7. Dunning, T. H., Gaussian-Basis Sets for Use in Correlated Molecular Calculations .1. the Atoms Boron Through Neon and Hydrogen. *Journal of Chemical Physics* **1989**, *90* (2), 1007-1023.
8. Vrcelj, R. M.; Sherwood, J. N.; Kennedy, A. R.; Gallagher, H. G.; Gelbrich, T., Polymorphism in 2-4-6 Trinitrotoluene. *Crystal growth & design* **2003**, *3* (6), 1027-1032.
9. Hakey, P.; Ouellette, W.; Zubieta, J.; Korter, T., Redetermination of cyclo-trimethylenetrinitramine. *Acta Crystallographica Section E: Structure Reports Online* **2008**, *64* (8), o1428-o1428.
10. Millar, D. I.; Oswald, I. D.; Barry, C.; Francis, D. J.; Marshall, W. G.; Pulham, C. R.; Cumming, A. S., Pressure-cooking of explosives—the crystal structure of ϵ -RDX as determined by X-ray and neutron diffraction. *Chemical communications* **2010**, *46* (31), 5662-5664.
11. Iuzzolino, L.; Reilly, A. M.; McCabe, P.; Price, S. L., Use of Crystal Structure Informatics for Defining the Conformational Space Needed for Predicting Crystal Structures of Pharmaceutical Molecules. *Journal of Chemical Theory and Computation* **2017**, *13* (10), 5163-5171.
12. Wilson, W. S.; Bliss, D. E.; Christian, S. L.; Knight, D. J. *Explosive properties of polynitroaromatics*; NAVAL WEAPONS CENTER CHINA LAKE CA: 1990.
13. Choi, C. S.; Abel, J. E., The Crystal Structure of 1,3,5-Trinitrobenzene by Neutron Diffraction. *Acta Crystallographica Section B - Structural Crystallography and Crystal Chemistry* **1972**, *28* (1), 193-201.
14. Carper, W. R.; Davis, L. P.; Extine, M. W., MOLECULAR-STRUCTURE OF 2,4,6-TRINITROTOLUENE. *Journal of Physical Chemistry* **1982**, *86* (4), 459-462.
15. Dobratz, B. M. *Ethylenediamine Dinitrate and its Eutectic Mixtures: A Historical Review of the Literature to 1982*; LOS ALAMOS NATIONAL LAB NM: 1983.
16. Storm, C. B.; Stine, J. R.; Kramer, J. F., SENSITIVITY RELATIONSHIPS IN ENERGETIC MATERIALS. *Chemistry and Physics of Energetic Materials* **1990**, *309*, 605-639.
17. Welch, G. W. A.; Karamertzanis, P. G.; Price, S. L.; Leslie, M. *DMACRYS, 1.05*, is a substantial revision of DMAREL; 2010.

18. Williams, D. E., Nonbonded Interatomic Potential-Energy Functions and Prediction of Crystal-Structures. *Acta Crystallographica Section A - Foundations of Crystallography* **1984**, *40*, C95-C95.